Far East Journal of Mechanical Engineering and Physics
Volume 1, Number 2, 2010, Pages 99-109
This paper is available online at http://pphmj.com/journals/fjmep.htm

SCALAR RELATIVISTIC AND IMPURITY EFFECTS ON NANO-InSb MIS CAPACITOR CHARACTERISTICS

H. SIMCHI, M. MEHMANDOOST, SH. MOHAMMADNEJAD, E. MAHMOODZADEH and M. H. SAANI

Semiconductor Component Industry (SCI)
P. O. Box 19575-199, Tehran, Iran

Nanoptronics Laboratory
Iran Science and Technology University
Tehran, Iran

Abstract

In this paper, we modeled a nano-InSb metal-insulator-semiconductor (MIS) capacitor with one dimensional Schrödinger-Poisson coupled equation in both nonrelativistic and scalar relativistic cases. We showed, the charge density is peaked near the middle of the channel in nonrelativistic case (called size quantization) and it disappears as we consider the scalar relativistic effects although we do not change the size. Consequently the electron distribution looks more classical for scalar relativistic case. Also we showed the existence of an effective coulomb (or parabola) like potential which can be created by an impurity, cleaning process of surface, insulator layer deposition, or misalignment in lithography process of gate, confines the electrons at surface and it means that the device always remains in the OFF regime. Therefore one may conclude that, in manufacturing nano-InSb MIS capacitor the cleaning process of InSb surface, growth process of insulator layer and lithography process of gate, are very important and critical processes. Also one should attend to classical behavior in characterization process of device although the size of device is in nanometer scale.

Keywords and phrases: nano-InSb MIS capacitor, Schrödinger-Poisson coupled equation, scalar relativistic effect, electron distribution, Fermi energy level.

Received March 6, 2010

1. Introduction

Starting about 20 years ago, advances in semiconductor technology allowed the fabrication of structures so small that their discrete quantum level structure was resolvable. In the past few years, powerful new spectroscopic probes have revealed a wealth of new physics in these “artificial atoms”. The spacing between atoms in a semiconductor crystal is typically about 0.3-0.4 nm. In artificial atoms, electrons are confines in structures about 100 nm in diameter. Thus, an artificial atom in a crystal comprises many real atoms and they are typically much larger than real atoms. Therefore the electron orbits do not simply scale with size. The separation in energy of the different orbits of electron in the artificial atom is another energy scale. As the atomic size increases, the differences in the orbital energies decrease faster than the coulomb energy. It follows that in a large atom, the effects of electron-electron interaction are relatively more important than in small atom. It may not be long before these distinctions affect modern electronics. As device shrink, it is already possible to create electronic devices small enough to have device characteristics sensitive to the motion of single electrons within them, even at room temperature [1, 2]. Building devices at this size scale that have reproducible and desired electronic properties will be an immense challenge. The single electron transistor (SET) relies on the discrete nature to modulate the conductance of small, isolated volume of conducting material. Within this nano scale region, known as a quantum dot, the confinement in all three dimensions is sufficiently strong that the electrons may only exist at well-defined quantized energies. The confining potential may be created either by the physical dimensions of the dot [3, 4, 5], or by inducing an electrostatic potential at the surface of a semiconducting hetero structure [6]. The use of the spin quantum number of a single confined electron has been demonstrated as a ‘quantum bit’ in such semiconductor systems [7]. Of all the III-V semiconductors InSb offers the smallest electron effective mass, the highest mobility and the largest g-factor. The large g-factor has important implication for potential spin-to-charge readouts of quantum bits [8] and also offers the possibility of localized quantum bit addressing [9]. *Therefore we studied InSb*. Generally quantum dot is located between two capacitor plates in vertical SET [4, 5]. It is close enough to one of the plates to allow single electrons to tunnel (or hope) between the artificial atom and the nearby plate. The artificial atom is far enough from the other capacitor plate to prohibit tunneling to this pale. But the generic structure of ‘nano transistor’ consists of a semiconductor channel separated by an insulator layer from metallic gate. The two contact pads are

source and drain and the resistance of the channel determines the current that flows from the source to the drain when a voltage is applied between them. The gate voltage is used to control the electron density in the channel and hence its resistance. If one shorts drain pad to source the quantum electron density function, along quantization axis, is very important function in studying the charge transport phenomena in FET. In fact after shorting the drain to source, the FET looks like a MIS quantum capacitor along quantization axis. *Therefore we studied quantum electron density of MIS capacitor*. But for studying the subject, one requires the self-consistent solution of the Schrödinger equation and the Poisson equation. A self-consistent solution of Schrödinger-Poisson equations using a nonuniform mesh was used for studying planar epitaxial structures [10]. A numerical Schrödinger-Poisson solver was used for studying radially symmetric nano wire core-shell structures [11]. Three dimensional self-consistent solutions of Poisson and Schrödinger equation was used for studying electrostatically formed quantum dot [12] and Boudib et al., used computational method for solving the Poisson-Schrödinger equation in studying the semiconductor field effect transistor nano structure [13]. *Therefore we used finite difference method for solving the Poisson-Schrödinger equation*. The effects of the optical response properties of InSb after including scalar relativistic zeroth-order regular approximation (ZORA) in the ground-state density functional theory, as well as in the time-dependent response calculations was studied by Kootstra et al. [14]. Also it was shown the overestimated values of band gap of InSb can be decreased by considering the relativistic effects and in some cases InSb crystal even to be a semimetal [14, 15]. In this article we modeled a nano-InSb metal-insulator-semiconductor (MIS) capacitor with one dimensional Schrödinger-Poisson coupled equation in both nonrelativistic and scalar relativistic cases. We showed, the charge density is peaked near the middle of the channel in nonrelativistic case (called size quantization) and it disappears as we consider the scalar relativistic effects although we do not change the size. Consequently the electron distribution looks more classical for scalar relativistic case. Also we showed the existence of an effective coulomb (or parabola) like potential which can be created by an impurity, cleaning process of surface, insulator layer deposition, or misalignment in lithography process of gate, confines the electrons at surface and it means that the device always remains in the OFF regime.

Therefore one may conclude that, in manufacturing nano-InSb MIS capacitor the cleaning process of InSb surface [16, 17], growth process of insulator layer [18] and lithography process of gate, are very important and critical processes. Also one

should attend to classical behavior in characterization process of device although the size of device is in nanometer scale.

2. Theory

An MIS capacitor comprises an InSb layer which was sandwiched between two insulator layers. The dimension in *x* and *y*-direction are enough large and in *z*-direction is enough small. Now the Schrödinger equation can be written as below in effective mass approximation [19]:

$$\left[E_c - \frac{\hbar^2}{2}\frac{\partial}{\partial z}\left(\frac{1}{m_c(z)}\frac{\partial}{\partial z}\right) + U(z) + \frac{\hbar^2}{2m_c(z)}(k_x^2 + k_y^2)\right]\phi_\alpha(z) = \varepsilon_\alpha\phi_\alpha(z), \quad (2.1)$$

where m_e is effective mass and $\hbar k_x$ and $\hbar k_y$ are momentum in *x* and *y* directions respectively. This is a one dimensional equation that can be numerically solved for given value of k_x and k_y. By replacing the kinetic-energy operator by the ZORA term [14]:

$$T_{ZORA}^{SR} = p \cdot \frac{c^2}{2c^2 - \nu_{eff}(z)}\, p \quad (2.2)$$

in which $p = -i\hbar\nabla$, c is the velocity of light, and $\nu_{eff}(Z)$ is the self-consistent effective potential, the ground-state ZORA equation is [14]:

$$\left[-\nabla \cdot \frac{\hbar^2 c^2}{2m_c c^2 - \nu_{eff}(r)}\nabla + \nu_{eff}(r)\right]\psi_\alpha = \varepsilon_\alpha\psi_\alpha. \quad (2.3)$$

Of course it should be solved in one direction (i.e. *z*-direction). The effective potential, v_{eff}, is lattice periodic and comprises the gate voltage, coulomb and exchange-correlation contributions.

The Poisson equation is:

$$\vec{\nabla} \cdot (\varepsilon_r \vec{\nabla} U) = -\frac{q^2}{\varepsilon_0}(n(\vec{r}) - n_0) \quad (2.4)$$

which ε_r is the relative permittivity, $n(r)$ and n_0 are electron density at point *r* and equilibrium respectively. Of course it should be solved in one direction (i.e. *z*-

direction) self-consistently with one dimensional Schrödinger equation (2.1) in nonrelativistic case and equation (2.3) in relativistic case.

The density matrix rho at equilibrium can be written as the Fermi function of the Hamiltonian matrix as below [14]:

$$\rho = f_0(H - \mu I), \tag{2.5}$$

where H is Hamiltonian, μ is Fermi energy (E_f) and I is the identity matrix of same size as H. It can be shown; the electron density is given by diagonal elements of rho [14]:

$$n(\vec{r}) = [\rho(\vec{r}, \vec{r}')]_{\vec{r}=\vec{r}'}. \tag{2.6}$$

3. Finite Difference Method

We considered the device with structure as insulator (3.75 nm)-InSb (2.5 nm)-insulator (3.75) in z-direction and the dimension in x and y-directions are enough large. The total dimension of device is 10 nm. We divided the 10 nm length to 200 pieces and therefore first insulator layer consists 75 pieces, InSb consists 50 pieces and second insulator layer consists 75 pieces. The length of each piece is 0.05 nm. The gate voltage is equal to 0.25V, and kT is equal to 0.025V. Also we assumed the bottom of conduction band, E_c, is equal to zero and three electron volts in semiconductor and insulators respectively and the electrochemical potential, μ, is equal to E_c.

For nonrelativistic case the Hamiltonian is [14, 20]:

$$H_{n,m} = [U_n + 2t_0]\delta_{n,m} - t_0\delta_{n,m+1} - t_0\delta_{n,m-1}, \tag{2.7}$$

where $t_0 = (hbar)^2/(2ma^2)$ and a is the length of each piece.

For relativistic case, one can show the equation is [20]:

$$[(D_{i+1/2} + D_{i-1/2})\phi_i - D_{i+1/2}\phi_{i+1} - D_{i-1/2}\phi_{i-1}] + \nu_{eff,i}\phi_i = \varepsilon_i\phi_i, \tag{2.8}$$

where

$$D_i = -\frac{\hbar^2 c^2}{2m_c a^2(2c^2 - \nu_{eff,i})} \tag{2.9}$$

and $D_{i+1/2} = \frac{1}{2}(D_i + D_{i+1})$ and $D_{i-1/2} = \frac{1}{2}(D_i - D_{i-1})$.

Also we can write the Poisson equation as below [14, 20]:

$$\varepsilon_r U_{n,m}[2\delta_{n,m} - \delta_{n,m+1} - \delta_{n,m-1}] = -\frac{q^2}{\varepsilon_0}(n_n - n_n^0). \quad (2.10)$$

We assumed the electrons are affected by a coulomb like potential, $1/r$ (or parabola like, $1/r^2$) in *z*-direction. The effective potential can be made by a positive impurity atom which is placed at center of the *z*-axis or at surface (or it may be made by fork-gate [21, 22]).

Therefore the effective potential comprises the gate voltage, and coulomb (parabola) like contributions. At first, we found the Hamiltonian matrix in both nonrelativistic and relativistic cases. Then we solved Schrödinger-Poisson coupled equation self-consistently and find rho matrix. The diagonal rho matrix is the electron density function.

4. Results and Discussion

The electron density function is shown in Figure 1a (nonrelativistic case) and 1b (relativistic case) and the equilibrium band diagram is shown in Figure 2a (nonrelativistic) and 2b (relativistic) when the impurity is at the center of *x* axis.

Also the electron density function is shown in Figure 3a (nonrelativistic case) and 4a (relativistic case) and the equilibrium band diagram is shown in Figure 3b (nonrelativistic) and 4b (relativistic) when the impurity is at the surface.

In nonrelativistic case, the energy levels in *z*-direction are quantized and the energy levels get closer together when we make the channel wider. Consequently the electron distribution looks more classical for wide channel [19]. Previously it was shown [14, 15] that the calculated band gap of InSb coincides more with experimental data (i.e. smaller band gap) when the scalar relativistic effect is added to Hamiltonian. In the other words, the overestimation will be decreased. Similarly one can assume when effective potential is placed at the center of the *z*-axis, in relativistic case the energy difference between neighborhood levels decreases in *z*-direction, and it makes the electron distribution looks more classical (similar to wide channel). In the other words the energy levels get closer together in this case. Therefore one may conclude that the classical behavior of device can be the reason for gate failure in reported works [22].

Now consider the effective potential is placed at surface. It can be done if some impurities atoms or dangling bands are place at the surface. Also if there is a misaligning in lithography process and fork-gate close to surface boundaries. As figures three and four show, the charge is confined at surface. It means that, the device always remains in OFF regime. It was shown that after cleaning the InSb surface the indium and antimony oxides are made on the surface [16, 17]. These compositions can create dangling energy levels in band energy diagram. Also it was shown the growth process of an insulator layer on InSb surface can creates dangling energy levels in band diagram [18]. Therefore these process or lithography can be the source effective potential at surface. Then one may conclude that the classical behavior of device can be the reason for gate failure in reported works [22].

5. Conclusion

In some previous works [22], the low yield of manufacturing process and gate failure mechanism were reported as main problems in manufacturing InSb SET. In this article we showed the importance of considering the scalar relativity effect in InSb [14, 15] can be considered as a source for these problems. In the other words, we added the scalar relativistic effect to Hamiltonian and showed the InSb MIS capacitor behaves as a classical capacitor although its total length is 10 nm. Also based on the results of reported works [15, 16, 17, 18] the cleaning process, and insulator deposition process can make dangling energy levels in band diagram. These effects and misalignment in lithography can be modeled by an effective potential at the surface of the device. In these cases we showed the electrons are confined at surface and the device always remains at the OFF regime.

References

[1] K. Yano et al., IEEE Int. Elect. Dev. Meeting in IEEE International Electron Devices Meeting 541-544, IEEE, New York, 1993.

[2] Y. Takahashi et al., Electron. Lett. 31 (1995), 136-137.

[3] E. Bar-Sadeh et al., Phys. Rev. B 50 (1994), 8961-4.

[4] M. T. Björk et al., Nano Lett. 4 (2004), 1621-25.

[5] J. Gorman et al., Phys. Rev. Lett. 95 (2005), 090502.

[6] J. H. Jefferson and W. Häusler, Preprint cond-mat/9705012, 1997.

[7] J. R. Petta et al., Science 309 (2005), 2180.

[8] F. H. L. Koppens et al., Nature 442 (2006), 766-71.

[9] M. T. Björk et al., Phys. Rev. B 72 (2005), 201307®.

[10] I-H Tan et al., J. Appl. Phys. 68(8) (1990), 4071-6.

[11] Lingquan Wang et al., Solid-State Electronics 50 (2006), 1732-1739.

[12] E. Machowska-Podsiadlo et al., Bulletin of the Polish Academy of Science, Technical Science 55(2) (2007).

[13] O. Boudib et al., African Phys. Rev. 2 Special Issue (Microelectronics): 0011, 2008.

[14] F. Kootstra et al., J. Chem. Phys. 114(4) (2001).

[15] H. Simchi et al., Comp. Matt. Sci. 40 (2007), 557-561.

[16] H. Simchi et al., Eur. Phys. J. Appl. Phys. 33 (2006), 1-4.

[17] H. Simchi et al., Infra. Phys. Tech. 52 (2009), 113-118.

[18] H. Simchi et al., Infra. Phys. Tech. 51(3) (2008), 263-269.

[19] S. Datta, Quantum Transport, Cambridge University Press, 2005.

[20] Steven E. Koonin and C. Dawn, Meredith ‘Computational Physics, Fortran Version’, Addison-Wesley Publishing Company, 1998.

[21] J. H. Davis et al., J. Appl. Phys. 77 (1995), 4504-12.

[22] J. M. S. Orr et al., New J. Phys. 9 (2007), 261.

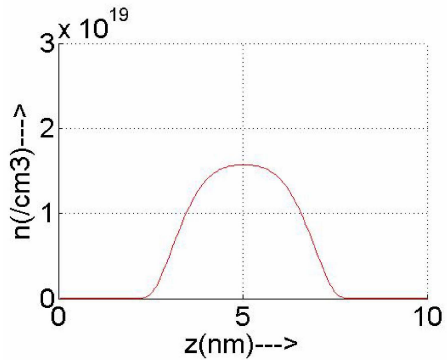

Figure 1a. Electron density in the case of nonrelativistic Hamiltonian including coulomb like potential (v_{eff} is at center).

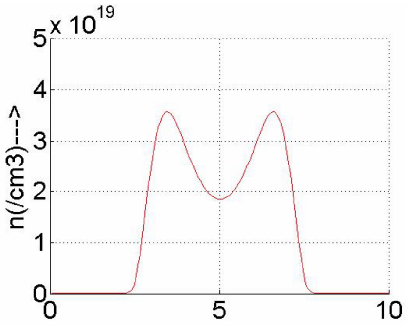

Figure 1b. Electron density in the case of scalar relativistic Hamiltonian including coulomb like potential (v_{eff} is at center).

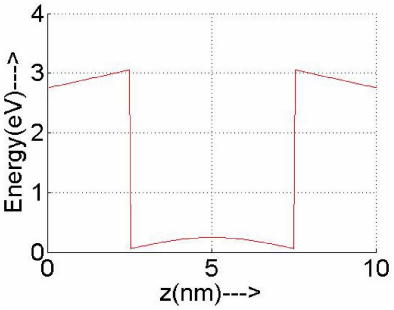

Figure 2a. The equilibrium band diagram in nonrelativistic case (v_{eff} is at center).

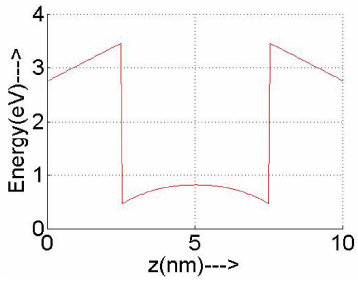

Figure 2b. The equilibrium band diagram in relativistic case (v_{eff} is at center).

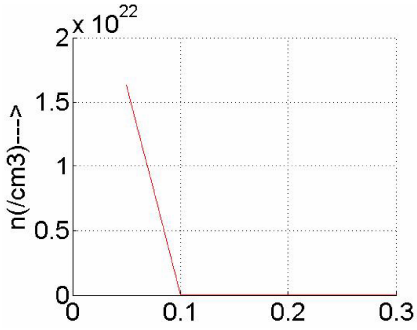

Figure 3a. Electron density in the case of nonrelativistic Hamiltonian including coulomb like potential (v_{eff} is at surface).

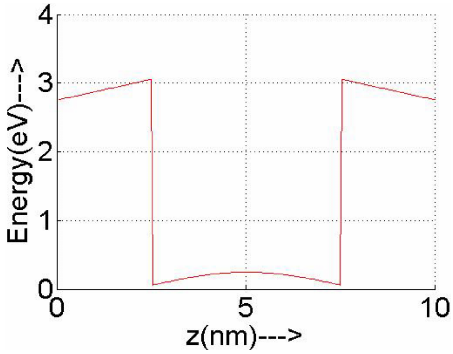

Figure 3b. The equilibrium band diagram in nonrelativistic case (v_{eff} is at surface).

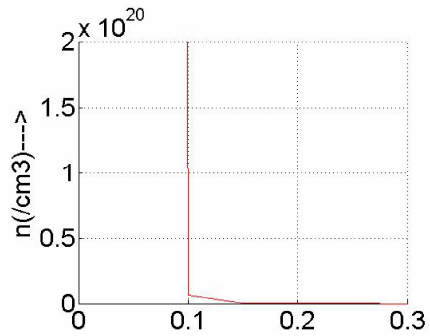

Figure 4a. Electron density in the case of relativistic Hamiltonian including coulomb like potential (v_{eff} is at surface).

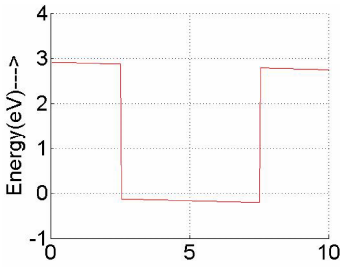

Figure 4b. The equilibrium band diagram in relativistic case (v_{eff} is at surface).